Acta Cryst. (1967). **22**, 406

Crystallographic Studies of Metal–Peptide Complexes. V. (β-Alanyl-L-histidinato)copper(II) Dihydrate

BY H. C. FREEMAN AND J. T. SZYMANSKI*
School of Chemistry, University of Sydney, Sydney, Australia

(*Received* 21 *December* 1965 *and in revised form* 13 *July* 1966)

Crystals of the copper(II)-carnosine complex, (β-alanyl-L-histidinato)copper(II) dihydrate, are trigonal, space-group $P3_12$, with $a=8{\cdot}641\pm0{\cdot}009$, $c=30{\cdot}576\pm0{\cdot}015$ Å, $Z=6$. The complex is a dimer in which each copper atom has coordination number 5. The four closest ligand atoms are the terminal amino nitrogen (1·96 Å), peptide nitrogen (1·95 Å) and carboxyl oxygen (1·93 Å) of one dipeptide molecule, and the 3-nitrogen of the imidazole ring of the second peptide molecule of the dimer (2·01 Å). Each dipeptide is thus bonded to two different copper atoms. The fifth ligand on each copper atom, completing a square-pyramidal environment, is a water molecule (2·48 Å). The dimers are linked by a hydrogen-bond network involving a second water molecule per formula unit. The atoms –N–C–C–CO– of the β-alanyl chelate ring are disordered in the crystal, indicating that the ring does not have a single preferred conformation. This disorder reduces the precision with which the rest of the molecule may be determined. The anisotropic full-matrix least-squares refinement converged with $R=0{\cdot}10$ for 1319 independent reflexions.

Introduction

Carnosine (β-alanyl-L-histidine) and its 1-methyl derivative, anserine, occur in the muscle fibres and various organ tissues of all vertebrates. It is the substrate of the metal-activated enzyme carnosinase, extensively discussed by Rosenberg (1960, 1961), but the biological function of carnosine has not yet been elucidated.

The preparation of crystals of a copper–carnosine complex from horse protein was first reported by Maunthner (1913). By analysis the complex was (erroneously) found to be a monohydrate. Proposals for its structure have been based mainly on *p*H-titration studies of carnosine in the absence and presence of copper(II) ion. Dobbie & Kermack (1955) proposed structure (I), the (at that time) novel feature of which was metal-binding at a peptide nitrogen atom from which the hydrogen had been dissociated. In structure (II), suggested (minus its H_2O molecule) by Martin & Edsall (1960), the imidazole ring was allowed to keep its aromatic character, this being consistent with stabilization of the metal–imidazole bond by $d_\pi-p_\pi$ donation. Martin (1960) preferred (I) in order to explain the identity of the titration curves of anserine and carnosine in the presence of copper(II) ion: anserine has a methyl group on the 1-nitrogen atom of the imidazole ring. Lenz & Martell (1964) calculated the stability constants for the proposed intermediates $CuLH^{2+}$ and CuL^+, and for CuL (where LH = carnosine); they showed (I) as the structure of CuL although everything in their paper seems equally consistent with (II). All these authors were in essential agreement that Cu^{II} is initially bound to the 1-nitrogen of the imidazole ring, and that the terminal NH_2 and de-protonated peptide nitrogen become binding sites as the *p*H is increased. Except in the early stages of complex formation (Lenz & Martell, 1964), the possibility of metal-binding at the carboxyl group has been completely discarded, presumably because it is impossible to build strainless models in which all four potential donor atoms of the dipeptide adopt a square-planar configuration about the copper. Lukton & Sisti (1961) used the infrared spectrum of the solid complex to prove that the carboxyl group is not involved in coordination.

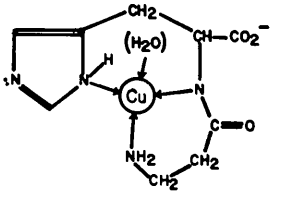

(I)

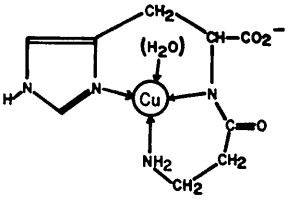

(II)

Histidyl residues are known to be important metal-binding sites in proteins. The crystal structure of the copper-carnosine complex has therefore been solved as part of a continuing study of model compounds for metal–protein interaction (Freeman, Robinson & Schoone, 1964; Freeman, Schoone & Sime, 1964; Freeman & Taylor, 1965; Blount, Fraser, Freeman, Szymanski & Wang, 1966). Neither (I) nor (II) correctly represents the structure of the complex in the solid state.

Experimental

Deep blue crystals of the complex were grown by allowing a concentrated alkaline solution of copper hy-

* Present address: Department of Chemistry, University of Toronto, Toronto 5, Canada.

droxide and carnosine to evaporate slowly to dryness. The crystals exhibited the trigonal rhombohedral forms $\{10\bar{1}1\}$ and less prominently $\{01\bar{1}1\}$ and the pinacoid form $\{0001\}$. The pinacoid faces showed a pronounced irregular concavity. The unit-cell dimensions a and c were fitted by least-squares to the values of $4\sin^2\theta/\lambda^2$ of 40 $h0l$ reflexions with $59° \leq \theta \leq 81°$, with corrections for absorption and eccentricity (Buerger, 1942). The spacings were measured on a Weissenberg photograph taken with the film mounted in the Straumanis position. The probable errors in a and c were taken arbitrarily as three times the standard deviations calculated from the least-squares matrix.

Crystal data

$C_9H_{16}O_5N_4Cu$ ($C_9H_{12}O_3N_4Cu.2H_2O$), F.W. 323·8.

Trigonal, $a=8{\cdot}641\pm0{\cdot}009$, $c=30{\cdot}576\pm0{\cdot}015$ Å.
$D_m=1{\cdot}65$, $D_x=1{\cdot}63$ g.cm^{-3}, $U=1977{\cdot}2$ Å^3, $Z=6$.
$\lambda(\text{Cu } K\alpha_1)=1{\cdot}5405$, $\lambda(\text{Cu } K\alpha_2)=1{\cdot}5443$ Å.

Space group $P3_12$ or $P3_22$, determined from systematic extinctions ($00l$ present only for $l=3n$) and from diffraction symmetry; $P3_12$ confirmed by structure analysis.

A crystal with maximum and minimum dimensions of 0·225 and 0·175 mm was selected for intensity estimation. Equi-inclination Weissenberg data were collected with Cu $K\alpha$ radiation using the multiple film technique for the layers $h=0$ to $h=5$ (integrated) and for the layers $h=0$ to $h=6$ (non-integrated). The integrated data were measured photometrically on both the top and bottom halves of each film. The non-integrated data were estimated visually by comparison with a standard scale, and were then scaled to the integrated data to provide values for the weaker intensities and those for which the $K\alpha$ splitting made photometry unreliable.

The diffraction symmetry ($\bar{3}m$) permitted a comprehensive correlation of intensities measured in the various layers, since a general reflexion row (*e.g.* $21\bar{3}l$ measured on the layer $h=2$) appears in symmetry-related rows ($12\bar{3}l$ on the layer $h=1$ and $3\bar{1}\bar{2}l$ on the layer $h=3$). The Lorentz–polarization–Tunell corrections were applied but no corrections for absorption were made. The standard deviation $\sigma(F^2)$ of each reflexion was obtained by taking into account the intensity range in which it was observed, the number of observations of the reflexion and its symmetry-related reflexions, and the probable errors in the layer scale factors. A total of 1319 independent reflexions were estimated, of which 135 were unobservably weak. These were assigned a value one half of the locally observable minimum intensity ($I_{\min}$) with a standard deviation of $I_{\min}/2\sqrt{3}$ (Hamilton, 1955).

The structure was solved in the space group $P3_12$, and the configuration of the histidine residue was found to agree with the known configuration of L-histidine (Langenbeck, 1925).

Structure determination

Considerable thermal diffuse scattering was observed on the $0kl$ films. The data extended much further in the **c*** than in the **a*** and **b*** directions. A Wilson plot using $hk0$, $hk1$ and $hk2$ reflexions indicated a temperature factor of $B\simeq10$–12 Å^2. In contrast, a sampling of reflexions of the type hkl (h, $k\leq2$) showed $B\simeq4{\cdot}5$ Å^2. Allowance for the apparent thermal anisotropy was made in a sharpened Patterson function†, which revealed the positions of the heavy-atom vectors. These were found to lie superimposed in pairs on the mirror planes in Patterson space. A Fourier map with phases calculated from the heavy-atom positions thus showed the structure superimposed upon its mirror image. Unambiguous identification of the light atom peaks was impossible, except for those on or very near the false mirror plane. A product synthesis (Fridrichsons & Mathieson, 1962) using coefficients of the type

$$[F_o(hkl)-F_c(hkl)]\,.\,F_c(hkl)\,.\,\exp i\alpha_c(hkl)$$

in a Fourier summation was calculated and compared with the heavy-atom Fourier synthesis. A comparison of peak heights and examination of the probable spatial distribution of peaks around the copper atom led to a tentative choice of nine light atom sites (one of which later proved incorrect). A Fourier synthesis using phases calculated from the copper atom and these nine light atoms revealed the whole structure.

Seven rounds of full-matrix least-squares refinement with anisotropic thermal parameters lowered R from 0·26 to 0·10. The maximum shifts at the end were about one-third of a standard deviation. The function minimized was $\Sigma w(|F_o|-|F_c|)^2$. The weights $w=1/\sigma^2(F)$ of both observed and unobservably weak reflexions were derived from the previously assigned standard deviations $\sigma(F^2)$ of the intensities. Intense inner reflexions which may have been affected by extinction (*e.g.* 003, 021, 111) were not omitted from the refinement since their weights were in any case small. Standard scattering factors were used for carbon, nitrogen, oxygen (*International Tables for X-ray Crystallography*, 1962*a*) and Cu^+ (*International Tables for X-ray Crystallography*, 1962*b*). From the latter curve 2·1 electrons were subtracted over the whole $\sin\theta$ range to allow for the real part of the anomalous scattering (Dauben & Templeton, 1955). The programs used for the refinement and molecular geometry calculations were ORFLS and ORFFE (Busing, Martin & Levy, 1962*a*, *b*).

The final positional and thermal parameters are listed in Tables 1 and 2, respectively. The atoms are labelled according to the following scheme:

† In the sharpening and modification function,

$$M(s)=(\Sigma Z_j^2/\Sigma f_j^2)(2\sin\theta/\lambda)^4\exp[-12(\sin\theta/\lambda)^2]\times\exp[0{\cdot}014(h^2+k^2+hk)],$$

the second exponential factor was introduced to compensate for the anisotropy in the data.

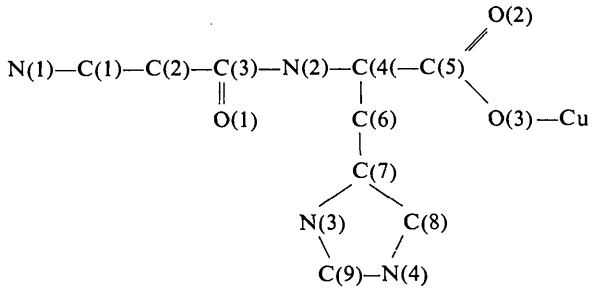

For ease of comparison, especially of the vibrational parameters (see below), the atoms are listed in these Tables in the same order as they occur in the molecule. The observed and calculated structure amplitudes are shown in Table 3.

Description of the structure

The structure consists of dimers (Figs. 1 and 2), whose dimensions are shown in Fig. 3 and Table 4. Each copper atom is bonded to the terminal amino nitrogen atom N(1), the deprotonated peptide nitrogen N(2), and a carboxyl oxygen O(3) of one carnosine molecule, and to the pyridine nitrogen N(4′) of the imidazole

Table 1. *The atomic positional fractional coordinates (with their standard deviations in parentheses)*

	$10^4x(10^4\sigma_x)$	$10^4y(10^4\sigma_y)$	$10^5z(10^4\sigma_z)$
Cu	4796 (03)	3196 (03)	29603 (04)
N(1)	7247 (19)	3636 (22)	29070 (31)
C(1)	8199 (28)	4152 (30)	24786 (48)
C(2)	7475 (29)	4244 (37)	20944 (51)
C(3)	5447 (17)	3546 (26)	20031 (33)
O(1)	4955 (14)	3377 (19)	16064 (24)
N(2)	4365 (15)	2953 (16)	23308 (24)
C(4)	2442 (15)	2011 (18)	22256 (33)
C(5)	1563 (24)	2296 (23)	26280 (41)
O(2)	−0194 (16)	1711 (20)	26107 (35)
O(3)	2495 (13)	3055 (19)	29690 (23)
C(6)	1690 (18)	0109 (18)	21165 (32)
C(7)	2050 (19)	−0971 (21)	24609 (31)
N(3)	3023 (16)	−1742 (18)	24035 (29)
C(8)	3020 (18)	−2616 (22)	27853 (36)
N(4)	1981 (16)	−2425 (15)	30763 (24)
C(9)	1299 (21)	−1436 (21)	28886 (32)
O(4)	6318 (13)	6430 (17)	31364 (32)
O(5)	2846 (20)	1326 (21)	09361 (34)

Table 2. *Anisotropic temperature factors and their standard deviations*

T.F. $= \exp[-\frac{1}{4}(B_{11}h^2a^{*2} + B_{22}k^2b^{*2} + B_{33}l^2c^{*2} + 2B_{12}hka^*b^* + 2B_{23}klb^*c^* + 2B_{13}hla^*c^*)]$

Atom	B_{11}	$\sigma(B_{11})$	B_{22}	$\sigma(B_{22})$	B_{33}	$\sigma(B_{33})$	B_{12}	$\sigma(B_{12})$	B_{23}	$\sigma(B_{23})$	B_{13}	$\sigma(B_{13})$
Cu	7·19	0·12	7·53	0·13	2·60	0·06	2·88	0·10	0·97	0·06	−0·24	0·06
N(1)	7·56	0·76	15·95	1·34	3·56	0·42	6·23	0·85	2·01	0·61	0·55	0·45
C(1)	10·14	1·27	14·13	1·39	4·88	0·63	6·22	1·16	1·81	0·78	0·15	0·73
C(2)	10·28	1·23	18·64	2·13	4·93	0·67	−5·67	1·57	3·83	1·06	−2·58	0·77
C(3)	5·03	0·61	12·99	1·30	2·56	0·38	1·05	0·91	2·16	0·57	0·59	0·38
C(1)	6·11	0·44	15·13	0·97	2·98	0·28	2·21	0·63	1·77	0·42	0·03	0·30
N(2)	6·89	0·58	8·81	0·70	1·79	0·26	3·24	0·58	1·03	0·34	0·05	0·31
C(4)	3·95	0·50	6·01	0·70	3·83	0·41	2·16	0·52	−0·75	0·41	−0·47	0·35
C(5)	9·67	1·08	8·33	0·91	3·63	0·53	3·25	0·83	0·99	0·54	−0·41	0·59
O(2)	6·85	0·61	12·42	0·97	7·38	0·55	5·30	0·68	−0·71	0·58	0·09	0·47
O(3)	6·96	0·52	6·84	0·51	4·01	0·29	3·48	0·44	0·19	0·31	−0·40	0·31
C(6)	5·93	0·66	6·73	0·72	2·90	0·36	3·25	0·59	0·70	0·40	0·53	0·39
C(7)	6·38	0·71	8·17	0·89	2·35	0·34	1·84	0·70	1·18	0·46	0·48	0·40
N(3)	6·53	0·64	8·22	0·75	3·14	0·35	4·54	0·59	0·98	0·42	1·25	0·38
C(8)	6·07	0·68	8·03	0·92	3·65	0·44	2·74	0·70	0·10	0·51	0·94	0·43
N(4)	7·50	0·65	7·41	0·62	2·00	0·28	3·61	0·54	0·15	0·32	0·67	0·33
C(9)	9·45	0·98	10·14	1·00	2·06	0·34	5·57	0·83	2·17	0·49	0·73	0·46
O(4)	5·10	0·47	10·68	0·79	6·83	0·48	2·59	0·58	0·82	0·48	0·33	0·37
O(5)	9·42	0·84	16·15	1·32	5·97	0·51	4·83	0·86	−2·91	0·67	−0·26	0·54

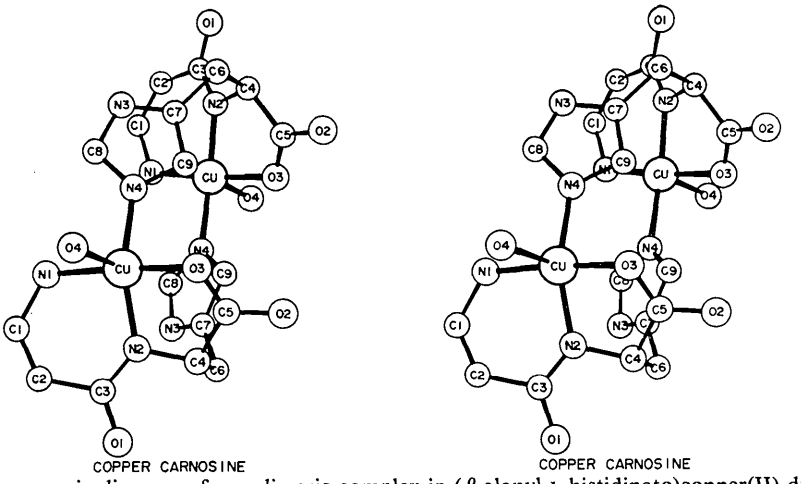

Fig. 1. Stereoscopic diagram of one dimeric complex in (β-alanyl-L-histidinato)copper(II) dihydrate.

Table 3. *Observed and calculated structure amplitudes*

Each line consists of the index l, $10|F_c|$, $10|F_o|$ and $10\sigma(F_o)$. Reflexions marked with T were unobservably weak.

ring of a second carnosine molecule. The two halves of this 'head to tail' dimer are related by a crystallographic twofold axis.

The coordination of the copper is approximately square-pyramidal. The four closest ligand atoms are displaced from a strictly square towards a flattened tetrahedral arrangement. Their average deviation from their plane of best fit (plane 1, Table 5) is 0·23 Å. The copper atom lies 0·13 Å from the same plane, in the direction of a water molecule O(4) in the fifth coordination position. The bond Cu–O(4) is not quite perpendicular to the plane of the four other ligands, but is bent in the direction of N(4′).

The Cu–N(4′) bond accommodates both the steric requirements of the copper atom and those imposed on the imidazole ring by its own peptide molecule. The deviation of N(4′) 'below' the base of the copper coordination pyramid corresponds to a deflection of the bond by about 6·2°; at its other end, the bond makes an angle of 5·4° with the imidazole plane, the distance of the copper atom from this plane being 0·19 Å. In addition to these two deflections, the imidazole ring is rotated about the Cu–N(4′) axis until the angle between the imidazole ring and the square of the four closest ligand atoms is 24°.

The angle between the normals to the 'coordination squares' of the two copper atoms of one dimer is 13·5°. The carboxyl group and the attached asymmetric carbon C(4) are co-planar. There are appreciable deviations from planarity in the peptide group C(2)C(3)O(1)–N(2)C(4) (mean deviation 0·050 Å, maximum 0·068 Å),

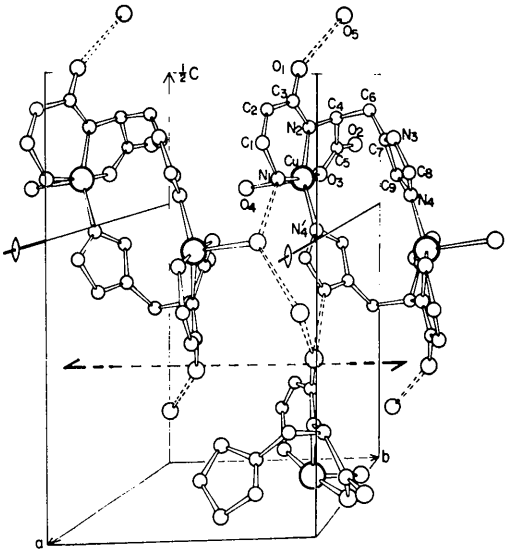

Fig. 2. Perspective drawing of part of (β-alanyl-L-histidinato)-copper(II) dihydrate structure. Two dimers in adjacent unit cells are shown.

Table 4(*a*). *Bond lengths and their standard deviations*

	Length *l*	σ(*l*)		Length *l*	σ(*l*)
Cu —N(1)	1·964 Å	0·014 Å	C(4)–C(5)	1·53 Å	0·018 Å
Cu —N(2)	1·952	0·007	C(5)–O(2)	1·34	0·019
Cu —O(3)	1·932	0·011	C(5)–O(3)	1·28	0·015
Cu —N(4′)	2·011	0·007	C(4)–C(6)	1·47	0·018
Cu —O(4)	2·483	0·013	C(6)–C(7)	1·54	0·018
N(1)–C(1)	1·49	0·018	C(7)–N(3)	1·32	0·019
C(1)–C(2)	1·36	0·022	N(3)–C(8)	1·39	0·016
C(2)–C(3)	1·55	0·025	C(8)–N(4)	1·33	0·012
C(3)–O(1)	1·27	0·012	N(4)–C(9)	1·38	0·014
C(3)–N(2)	1·29	0·013	C(9)–C(7)	1·43	0·013
N(2)–C(4)	1·48	0·015			

Table 4(*b*). *Bond angles and their standard deviations*

	Angle θ	σ(θ)		Angle θ	σ(θ)
N(1)–Cu —N(2)	93·9°	0·4°	N(2)–C(4)–C(5)	104·4°	1·0°
N(1)–Cu —O(3)	172·3	0·6	N(2)–C(4)–C(6)	114·4	1·0
N(1)–Cu —N(4′)	97·5	0·5	C(5)–C(4)–C(6)	112·6	1·1
N(2)–Cu —O(3)	82·6	0·4	C(4)–C(5)–O(2)	117·9	1·2
N(2)–Cu —N(4′)	156·6	0·6	C(4)–C(5)–O(3)	120·1	1·4
O(3)–Cu —N(4′)	88·2	0·5	O(2)–C(5)–O(3)	122·0	1·4
O(4)–Cu —N(1)	83·5	0·5	C(5)–O(3)–Cu	112·7	1·0
O(4)–Cu —N(2)	107·5	0·4	C(4)–C(6)–C(7)	114·3	1·0
O(4)–Cu —O(3)	91·0	0·4	C(6)–C(7)–N(3)	126·1	1·0
O(4)–Cu —N(4′)	94·1	0·5	C(6)–C(7)–C(9)	126·6	1·5
Cu —N(1)–C(1)	120·8	1·0	N(3)–C(7)–C(9)	107·1	1·3
N(1)–C(1)–C(2)	124·7	2·0	C(7)–N(3)–C(8)	109·5	1·0
C(1)–C(2)–C(3)	127·0	1·7	N(3)–C(8)–N(4)	108·2	1·3
C(2)–C(3)–O(1)	117·6	1·1	C(8)–N(4)–C(9)	108·8	0·8
C(2)–C(3)–N(2)	117·5	1·2	C(8)–N(4)–Cu′	127·4	1·0
O(1)–C(3)–N(2)	124·2	1·2	C(9)–N(4)–Cu′	123·6	1·0
C(3)–N(2)–C(4)	116·3	0·9	N(4)–C(9)–C(7)	106·3	1·3
C(3)–N(2)–Cu	131·4	0·9			
C(4)–N(2)–Cu	112·1	0·7			

Table 5. *Hydrogen bonds*

Code for superscripts:

′ = atom at $x-y$, $-y$, $\frac{2}{3}-z$	iv = atom at $1+(x-y)$, $1-y$, $\frac{2}{3}-z$
″ = atom at $x-y$, $1-y$, $\frac{2}{3}-z$	v = atom at $1-x$, $y-x$, $\frac{1}{3}-z$
‴ = atom at $1-x$, $1+(y-x)$, $\frac{1}{3}-z$	vi = atom at $-x$, $y-x$, $\frac{1}{3}-z$

(*a*) Hydrogen bond lengths (e.s.d. = 0·2 Å)

O(1)···H–O(5)	O(5)–H···O(1)	2·73 Å
O(1)···H–N(3‴)	N(3)–H···O(1v)	2·67
O(2)···H–O(5vi)	O(5)–H···O(2vi)	2·66
O(3)···H–O(4″)	O(4)–H···O(3iv)	3·04
O(4)···H–N(1″)	N(1)–H···O(4iv)	3·00
O(4)–H···O(5‴)	O(5)···H–O(4v)	2·74

(*b*) Bond angles at hydrogen-bonded atoms

C(3)———O(1)···H–O(5)	150·4°
C(3)———O(1)···H–N(3‴)	126·3
O(5)–H ····O(1)···H–N(3‴)	80·3
C(5)———O(2)···H–O(5vi)	128·7
Cu———O(3)···H–O(4″)	144·6
C(5)———O(3)···H–O(4″)	102·3
Cu———O(3)——C(5)	112·7
Cu———O(4)···H–N(1″)	98·3
O(5‴)···H–O(4)–H···O(3iv)	116·4
O(5‴)···H–O(4)···H–N(1″)	119·2
O(3iv)···H–O(4)···H–N(1″)	105·7
Cu———O(4)–H···O(5‴)	111·7°
Cu———O(4)–H···O(3iv)	102·9
O(1) ····H–O(5)–H···O(2vi)	114·9
O(1) ····H–O(5)···H–O(4v)	130·6
O(2vi)···H–O(5)···H–O(4v)	106·7
Cu———N(1)–H···O(4iv)	134·6
C(1)———N(1)–H···O(4iv)	104·6
Cu———N(1)———C(1)	120·8
C(7)———N(3)–H···O(1v)	130·0
C(8)———N(3)–H···O(1v)	120·3
C(7)———N(3)———C(8)	109·5

Table 6. *Planes of best fit* (*least squares*)

(*a*) Coefficients

Each plane is represented by $AX+BY+CZ+D=0$, where X, Y, Z are orthogonal coordinates obtained from the fractional coordinates x, y, z by the transformations

$$X=ax-\tfrac{1}{2}by,\ Y=\tfrac{1}{2}\sqrt{3}by,\ Z=cz$$

Plane	Description	*A*	*B*	*C*	*D*
1	Four donor atoms	0·1178	−0·9862	−0·1162	2·9574
2	Imidazole	−0·4317	−0·8341	−0·3434	2·9027
3	Peptide group	0·4337	−0·8964	−0·0912	1·4920
4	Peptide group	0·4976	−0·8659	−0·0511	1·0336
5	Carboxyl group	−0·2884	0·8884	−0·3571	1·4500
6	β-Alanine	0·3462	−0·9286	−0·1337	2·1197

(*b*) Deviations from planes*

Plane	1	2	3	4	5	6
Cu	(−0·127)	(−0·188)	(−0·279)	(−0·124)	(−0·454)	(−0·354)
N(1)	−0·206					0·029
C(1)						0·053
C(2)			0·061	(0·251)		−0·089
C(3)			−0·068	0·003		−0·064
O(1)			0·002	−0·001		0·093
N(2)	0·244		0·057	−0·002		−0·021
C(4)			0·061	−0·001	−0·001	(0·243)
C(5)					0·004	
O(2)					−0·001	
O(3)	−0·254				−0·002	
C(6′)		0·002				
C(7′)		−0·021				
N(3′)		0·014				
C(8′)		−0·004				
N(4′)	0·217	−0·005				
C(9′)		0·014				

* Atoms in parentheses were *not* included in the calculation of the plane.

but the positions of C(2), C(3) and O(1) are undoubtedly affected by disorder (see below).

An extensive network of hydrogen bonds links the dimers. The water molecule O(4) bonded to the copper atom is hydrogen-bonded to a second water molecule O(5‴), to the carboxyl oxygen atom O(3^{iv}) of another dimer and to the terminal amino nitrogen N(1″) in a third dimer. The free water molecule O(5) forms hydrogen bonds with O(4^{v}), with the carbonyl oxygen atom O(1) and with a carboxyl oxygen O(2^{vi}). The carbonyl oxygen atom O(1) accepts a hydrogen bond from a neighbouring pyrrole nitrogen N(3‴). The allocation of hydrogen atoms in these bonds is shown in Table 6, which also lists the hydrogen-bond lengths and angles.

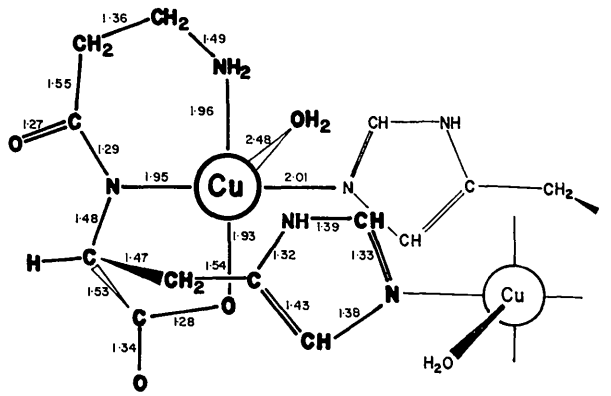

(*a*)

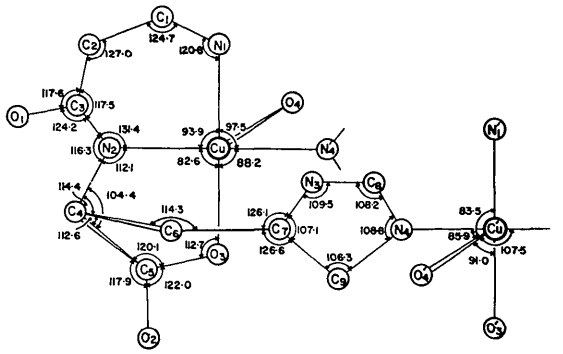

(*b*)

Fig. 3. (*a*) Bond lengths and (*b*) bond angles in (β-alanyl-L-histidinato)copper(II) dihydrate. The 'free' water molecule O(5) is not shown.

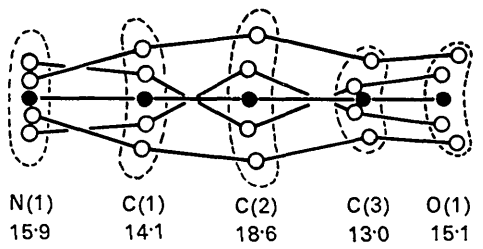

Fig. 4. Atomic sites (open circles) in four possible conformations of the β-alanine chelate ring. Full circles represent the positions found by least squares. Numbers below the atom designations are the values of B_{22}. The dashed lines indicate average electron density.

Discussion of the structure

The precision of this analysis is reduced by two effects. The first of these is a very strong correlation between the x and y coordinates of all atoms. Even within the correspondingly wider limits of accuracy, the structure has some apparently unacceptable features. The atoms N(1), C(1), C(2), C(3), O(1) of the β-alanyl chain and the water oxygen atom O(5) have abnormally large thermal vibration parameters B_{22} in directions approximately normal to the plane of the six-membered chelate ring. In this ring, the bond C(1)–C(2) is too short (1·36 Å) and the bond angles at C(1) and C(2) are larger than expected (127·0°, 124·7°). These effects are consistent with disorder in the buckling of this chelate ring.

Four possible conformations of the β-alanine chelate ring are illustrated in Fig. 4. All of them pivot about the copper atom and the peptide nitrogen N(2) which, being also part of the adjacent stable five-membered chelate ring, show no symptoms of disorder (B_{22} = 7·5, 8·8 Å^2). There are no close contacts on either side of the β-alanyl ring which might favour any particular conformation.

The very large thermal parameters obtained in the least-squares refinement therefore correspond to a smearing-out of the electron density perpendicular to the chelate ring, both because the atomic positions are disordered and because the maximum thermal vibrations are out-of-plane motions. The larger atomic vibration amplitudes in directions normal to **c** are expected, since these are the directions of weak binding in the crystal structure. The same explanations obviously apply (i) to the large value (16·1 Å^2) of B_{22} for the free water molecule O(5), and (ii) to the apparently abnormal bond angles at both ends of the hydrogen bond between O(5) and the disordered O(1). Neither this hydrogen bond nor the other two involving O(5) lie in the direction of the maximum thermal vibration of O(5).

The effects of conformational disorder appear not to be localized at the disordered atoms. It seems logical to expect molecular and lattice relaxation effects about the imperfections. In the present structure these seem to be reflected especially in two unsatisfactory bond lengths in parts of the structure which show no disorder [C(4)–C(6), 1·47 Å; C(5)–O(2), 1·34 Å].

In an effort to correct for the effects of disorder, the refinement was repeated, the disordered chain being represented by half-atoms 0·5 Å apart. The shifts of some of these atoms were of the order of 1 Å and physically meaningless. After the event it was apparent that for 0·5 Å resolution, high-angle data would have been required. In the appropriate direction, however, the observably strong reflexions were limited to $\theta < 70°$ owing to the very disorder which higher-angle data were

needed to resolve. We note, finally, that evidence for exactly the same kind of disorder has been found by Prout & Wiseman (1964) in the structure of di[*cyclo*-hexane-1,2-dioximato(1-)]di-imidazoleiron(II) hydrate. In this structure, too, a six-membered ring (cyclohexane) has a number of conformers which could not be resolved in the refinement.

A final $(F_o - F_c)$-synthesis contained no positive or negative features exceeding 0·5 e.Å^{-3}. Some of the details were clearly spurious. No physical significance was therefore attached to positive peaks which occurred at most of the positions where hydrogen atoms were expected, nor to negative troughs at the sites of the disordered atoms which were bounded by slightly positive regions.

Chemical significance

Comparison with related structures

In this section we shall further develop some of the generalizations made in part IV of this series (Blount, Fraser, Freeman, Szymanski & Wang, 1967). The comparisons to be made here are with (i) bis-imidazolatocopper(II) (Jarvis & Wells, 1960; Freeman, 1966); (ii) bis-L-histidinatozinc(II) dihydrate (Kretsinger, Cotton & Bryan, 1963), bis-DL-histidinatozinc(II) pentahydrate (Harding & Cole, 1963), and the bishistidinato complexes of nickel(II), cobalt(II) and cadmium(II) (Fraser, Long, Candlin & Harding, 1965); (iii) glycylglycinatocopper(II) trihydrate (Strandberg, Lindqvist & Rosenstein, 1961), which is formed under similar conditions to the present complex; and (iv) (glycyl-L-histidinato)copper(II) sesquihydrate (Blount *et al.*, 1967). Appropriate abbreviations will be used in the following discussion.

Cu^{II}-imidazole bonds occur in $Cu(Im)_2$, Cu(Gly-His).$1\frac{1}{2}H_2O$ and in the present complex, Cu(βAla-His).$2H_2O$. Remembering that in $Cu(Im)_2$ there are two crystallographically distinct types of Cu atom and four distinct types of Cu–imidazole bond, we have six examples of $Cu–N_{Im}$ bonds. Their lengths range from 1·96–2·00 Å in $Cu(Im)_2$ and 2·00 Å in Cu(Gly-His).$1\frac{1}{2}H_2O$ to 2·01 Å in Cu(βAla-His).$2H_2O$. In all three complexes, the Cu atoms deviate from the imidazole planes (0·17–0·53 Å, 0·47 Å and 0·19 Å, respectively, corresponding to angles of 5·0–15·4°, 13·8° and 5·4° between the Cu–N bonds and imidazole planes). Steric strains are further accommodated by rotating the imidazole rings about the Cu–N bonds, and by distorting the coordination-square of the four closest donor atoms in the sense of a tetrahedron. The angles between the imidazole planes and the planes fitted to the four closest ligands range from 24° in the present complex to 75° for one of the imidazole rings in $Cu(Im)_2$. The bond directions at the nitrogen atoms and the orientations of the imidazole rings are not correlated with the extent to which the environments of the Cu atoms are tetrahedrally distorted. It has been noted in part IV (Blount *et al.*, 1967) that the same flexibility characterizes the imidazole–metal binding in Zn(L-His)$_2$.$2H_2O$, Zn(DL-His)$_2$.$5H_2O$ and Ni(DL-His)$_2$.$2H_2O$.

These comparisons lead to two structural generalizations. The first is that imidazole–metal coordination is remarkably flexible in adjusting to external forces (ring strain, non-bonded contacts). The deviation of the metal–N bond at the imidazole nitrogen atom from strict coplanarity with the ring is such a marked feature, and the orientation of the imidazole plane with respect to the metal atomic orbitals seems to be determined to such an extent by external forces, that $d_\pi - p_\pi$ electron donation can have but little importance in stabilizing the bonding.

On the other hand, no matter at which imidazole nitrogen atom any of these metals is bound, the aromaticity of the imidazole ring is preserved. If a metal atom is attached to one nitrogen atom of the ring, then a hydrogen atom, if any, is attached to the other nitrogen atom. Neither in the Cu(βAla-His).$2H_2O$ nor the Cu(Gly-His).$1\frac{1}{2}H_2O$ structures, nor in a single metal–histidine or metal–imidazole complex has the metal atom been found at a 4-covalent imidazole nitrogen atom. The structural evidence therefore points to the preservation of the resonance energy of the imidazole group as an important influence on the binding in this whole class of complexes.

A third important structural influence enables us to understand the differences between the structures of Cu(Gly-His).$1\frac{1}{2}H_2O$ and Cu(βAla-His).$2H_2O$. The absorption spectra of Cu^{II}–peptide complexes indicate that the order of the ligand-field effects among nitrogen donors is amino > peptide > imidazole (Bryce & Gurd, 1966). Since the copper(II) ion is sensitive to crystal-field stabilization, it has the greatest affinity for donor atoms with strong ligand-field effects (Orgel, 1960). Accordingly, in each of these two dipeptide complexes the amino and peptide nitrogen atoms are Cu-binding sites (the latter at *p*H's where its proton is dissociated). Each ligand molecule then presents the metal with the choice of using a carboxylic oxygen (to form a five-membered chelate ring) or the imidazole 1-nitrogen atom (to form a six-membered chelate ring) as the third donor atom in the coordination square. Since nitrogen atoms are characteristically better donors than oxygen in bonds to Cu atoms (Orgel, 1960), Cu(Gly-His).$1\frac{1}{2}H_2O$ forms a six-membered ring including the imidazole group. In the present complex, a six-membered ring already exists once the amino and peptide nitrogen atoms are involved. Metal-binding at the imidazole 1-nitrogen atom would create a second six-membered ring adjacent to the first. This would place excessive strains on the peptide nitrogen atom N(2). As it is, the internal angle at N(2) in the β-alanyl ring is near 130°; in Cu(Gly-His).$1\frac{1}{2}H_2O$, the internal angle at N(2) in the ring containing the imidazole group is 127°. The bonds at N(2) cannot accommodate these conflicting requirements of two six-membered rings and still preserve the planarity (and hence the resonance energy) of the peptide group. In Cu(βAla-His).$2H_2O$, the third donor

in the coordination square is therefore a carboxylic oxygen atom. Since the imidazole group (like the carboxyl group in Cu(Gly-His).$1\frac{1}{2}H_2O$) now cannot come within a bonding distance of the Cu atom, it exercises its strong donor properties by binding – at its 3-nitrogen atom – a Cu atom not attached to the rest of its own dipeptide molecule. The type of complex which is formed is seen to depend on the preservation of the approximately planar, trigonal arrangement of the bonds about the peptide nitrogen.

In binding Cu^{II} at the amino and peptide nitrogen and carboxylic oxygen atoms of the main peptide chain, β-alanyl-L-histidine resembles glycylglycine. The Cu–ligand bonds in Cu(βAla-His).$2H_2O$ are shorter than the corresponding bonds in the coordination squares of CuGG.$3H_2O$ (which has two complexes in the asymmetric unit). The resultant slightly higher ligand field is reflected in the longer bond to the apical water molecule (2·48 Å *versus* 2·30, 2·41 Å), following a trend discussed elsewhere (Freeman, 1966).

Three structure analyses of complexes containing β-alanyl–metal chelate rings have been published (Tomita, 1961; Bryan, Poljak & Tomita, 1961; Jose, Pant & Biswas, 1964). We resist the temptation to make comparisons between their dimensions and conformations and those of the disordered β-alanyl ring in Cu(βAla-His).$2H_2O$.

*Deductions from the infra-red spectrum**

From the reported method of preparation, there is little doubt that the solid investigated by Lukton & Sisti (1961) and the present complex are identical. The assignment of infrared absorption frequencies by these authors is based on the statement that 'the presence of unchanged carboxylate absorption maxima in the copper chelates ... strongly indicates that the carboxylate anion is not involved in the chelate'. As pointed out by Nakamoto (1963*a*), the observed ranges of frequencies for ν(COO–Cu) and ν(COO^- free) overlap each other. The use of infrared spectroscopic data as an indication of carboxyl-binding by a divalent metal ion in a solid compound is therefore risky. In Lukton & Sisti's study it leads to a demonstrably incorrect conclusion, since the crystal structure analysis shows that the carboxyl group *is* involved in the chelate.

The three bands recorded by Lukton & Sisti may be re-assigned in a way which, even if it does not prove anything, is at least consistent with the actual structure. With the reservation noted above, the maxima at 1407 and 1562 cm^{-1} correspond to the symmetric and antisymmetric stretching frequencies of the $-COO^-$ groups of many bis-amino acid chelates where the carboxyl groups participate in chelation (Nakamoto, 1963*b*). We note especially the identity of the above maxima with $\bar{\nu}$=1401, 1562 cm^{-1} in the spectrum of crystalline bis-β-alaninatocopper(II) hexahydrate, whose crystal structure is known (Tomita, 1961).

For the copper-carnosine band at 1618 cm^{-1}, there are three possible assignments, each of which is consistent with an established feature of the structure: (i) as a C=O band of the metal-binding carboxyl group, by analogy with this description of the 1618 cm^{-1} bands in the anhydrous glycine, alanine, sarcosine, proline and serine complexes of copper(II) (Rosenberg, 1956); (ii) as $\delta(NH_2)$, in agreement with Nakamoto's assignment for the 1605 cm^{-1} band in bisglycinatocopper(II); or (iii) as an amide C=O band shifted from 1656 cm^{-1} as a result of metal-binding at the amide nitrogen, as suggested by Lukton & Sisti. Assignment (i) is doubtful, since it is now apparent that the antisymmetric carboxylate C=O frequency does not shift much when the carboxyl group is coordinated to a divalent metal ion (Martell, personal communication). An experimental distinction between (ii) and (iii) could be made by deuterating the complex. Assignment (iii) can be explained because the electron shift to the metal is smaller than that to the peptide proton which Cu^{2+} replaces. The peptide oxygen therefore becomes more negative, the $C{-}O^{\delta-}$ bond-order is lower, and the peptide carboxyl frequency decreases. This line of reasoning is supported by the fact that peptide groups whose nitrogen atoms are metal-binding sites have significantly longer C=O and shorter C–N bonds than free peptide groups (Freeman, 1966). The relevant bond lengths in the present structure conform to this pattern [d(C=O)=1·27, d(C–N)=1·29; average in peptides, 1·23 and 1·32 Å], but are subject to the uncertainties mentioned earlier.

Finally, we note that the absence of the carnosine 1587 cm^{-1} band in the spectrum of the complex is consistent with the confirmed existence of a $Cu{-}NH_2$ bond.

Reinterpretation of solution data

The crystal structure differs in three respects from all the structures which have been proposed for the copper–carnosine complex in solution: (i) The complex exists in the crystal as a dimer, (ii) the copper(II) is bound at the imidazole 3-nitrogen atom instead of the 1-nitrogen, and (iii) the carboxyl group is involved in chelate formation. We assume that the dimeric complex is not formed by a major molecular rearrangement at the instant of crystallization. *Either* dimerization is inherent in the interaction between carnosine and copper, *or* the dimer is in equilibrium with a monomer and crystallizes because it is the predominant and/or least soluble species in the solution. At least the first of these alternatives seems to be compatible with the existing solution data.

It is worth recalling the comment of Leberman & Rabin (1959) on their own detailed study of the copper–histidine system: 'adequate agreement [between observed formation curves and those calculated from assumptions concerning the form of the ligand species] does not *prove* the correctness of the postulates made'.

* This section incorporates a number of suggestions kindly communicated by Prof. A. E. Martell after reading a draft of the manuscript.

This warning is relevant to the present discussion. Despite the self-consistency of the interpretation of the solution data for copper–carnosine, it is not unique. Each of the solution studies of the copper–carnosine system appears to have been carried out at only one total-metal concentration. This makes it impossible to eliminate or confirm dimer formation by applying the usual test for invariance of the 'formation curve' (plot of ligand number *versus* ligand concentration) with respect to total-metal concentration (Rossotti & Rossotti, 1961). Conversely, the existing equilibrium data for copper-carnosine should be as compatible with the existence of dimeric, as with that of monomeric, species. This will be assumed in the following discussion. We note, in passing, the occurrence of dimeric species in solutions of other dipeptides (Koltun, Fried & Gurd, 1960; Bryce, Pinkerton, Steinrauf & Gurd, 1965).

It has been clear since the work of Dobbie & Kermack (1955) that at alkaline *p*H's carnosine binds copper(II) at the terminal amino group, deprotonated peptide nitrogen and an imidazole nitrogen, and that the imidazole ring participates at an early stage of the reaction (*i.e.* as the *p*H is raised). Martin & Edsall (1960) specifically identified the 'pyridine' nitrogen (=N–) and not the 'pyrrole' nitrogen (–NH–) of the imidazole ring as the initial copper(II)-binding site; they chose, however, the tautomer with hydrogen on the 3-nitrogen as the reacting species, so that the metal must be attached at the 1-nitrogen atom. Even so, they stated that 'in the *p*H region where both the imidazole and amino groups are predominantly in the basic form, the metal will be more evenly distributed between the two sites. Little chelation is likely at either site as it would involve the formation of seven-membered or even larger rings! These statements seem to remain just as valid if the metal is bound at the imidazole 3-nitrogen atom. (Indeed, the second statement then applies *a fortiori*.) Furthermore, if the metal is 'distributed between the two sites' early in the reaction, it may happen that one metal atom becomes bonded to the amino group of one dipeptide and to the imidazole group of another, or that one dipeptide molecule binds two different copper atoms. The course proposed for the subsequent chelation remains unchanged. As the *p*H is raised the peptide nitrogen atoms are de-protonated, and complex formation by each dipeptide molecule continues as though the copper-binding side chain were not present. This is a process which can lead to dimerization without involving any change in the *p*H-titration curve.

This re-interpretation of the sequence of reactions proposed by Martin & Edsall overcomes one specific difficulty. In anserine, the imidazole 1-nitrogen atom is methyl-substituted. On the assumption that a chelate ring is formed and that this requires metal-binding at the 1-nitrogen atom, Martin (1960) found himself forced to write this nitrogen atom as 4-covalent. The identity of the titration curves of anserine and carnosine in the presence of copper(II) then implied that in the copper(II)-carnosine complex the 1-nitrogen is also 4-covalent (*i.e.* bonded to hydrogen as well as to the metal). If, however, the initial assumption is not made and the imidazole group is allowed to complex independently of the rest of the peptide, then metal-binding at the 3-nitrogen in anserine must be preferred because this preserves the aromaticity of the imidazole ring. The identity of the titration curves *then* becomes strong evidence that in solutions of carnosine, too, the metal is bound at the 3-nitrogen.*

We have stressed the connexion between the assumption that carnosine must form a chelate ring between the imidazole and amide groups, and the acceptance of the imidazole 1-nitrogen as the donor atom. The present crystal structure analysis not only shows that this assumption is invalid, but also suggests why it is invalid. The formation of two six-membered chelate rings sharing the amide nitrogen is improbable, for the geometrical reasons discussed earlier. These reasons and their consequences should be just as applicable in solution as in the solid state.

The same assumption is implicit in the sequence of copper-carnosine reactions proposed by Lenz & Martell (1964). The major practical contribution of these authors was the provision of comparative data on the titration behaviour of carnosine in the presence of a number of other metals in addition to copper(II). The preceding discussion applies also to the equilibria fitted to these data. Quite apart from the general question whether any of the postulated complexes actually exist

---

* The authors are indebted to Dr R. B. Martin for permission to quote the following personal communication: 'The titration curve for the 2:1 anserine-cupric ion solution presented in Fig. 1 of the cited paper by Martin (1960) clearly shows that only one of the two available anserine molecules is bound to each cupric ion. On the addition of the fourth and fifth equivalents of base, the second anserine molecule titrates with pK_a values which are nearly the same as those found in the absence of cupric ion.

'This result prompted me to titrate a solution containing carnosine and cupric ion in a 2:1 ratio. Again one carnosine molecule is bound to the metal ion and the other remains free in solution with normal pK_a. This result is the expected one for the dimer structure because all four nearly planar positions about the cupric ion are occupied by ligand groups, while at least one position is vacant or occupied by water in all proposed monomer structures. This last position should be the site of the additional ligand molecule in 2:1 mixtures, with a consequent decrease to lower *p*H in the titration curve. Since the second ligand molecule per cupric ion titrates normally, the inference is strong that no vacant site about the cupric ion is available, a result which the dimer structure accommodates. The freely titrating extra ligand is found only in solutions of carnosine or anserine with cupric ion and not with nickel ion, as shown by published titration curves (Martin, 1960).

'Recent measurements have also shown that the circular dichroism of a solution containing the uncharged 1:1 Cu^{II}-carnosine complex is unaffected from 230 to 710 mμ if a second equivalent of carnosine is added. If glycyl-histidine is used as the ligand, a similar experiment causes a considerable change in the circular dichroism in the ultraviolet region. Once again the inference is strong that Cu^{II} is fully coordinated in the carnosine complex but not in the glycyl-histidine complex'.

in the solution, however, the structural formulae for Lenz and Martell's $CuLH^{2+}$, CuL^{+} and CuL (LH = carnosine) seem to require modification. In all three formulae, the metal atom is shown bonded to a 4-covalent, protonated imidazole nitrogen atom. There now exists considerable structural evidence (see *Comparison with related structures*) against the occurrence of this type of coordination. In addition, in CuL^{+} the metal is shown attached to a peptide nitrogen atom at a *p*H where the latter has not yet lost its proton. Not only the resonance energy of the imidazole ring, but also that of the peptide group, would be sacrificed in the proposed structure. It was first stressed by Rabin (1956, 1958) that, prior to the dissociation of the peptide proton, the peptide resonance energy is conserved if metal-binding occurs not at the nitrogen but at the oxygen of the peptide group. Metal-binding at a protonated peptide nitrogen atom has indeed not been found in any crystal structure, whereas metal atoms are bound at peptide oxygen atoms both in glycylglycylglycinato-copper(II) sesquihydrate (Freeman, Robinson & Schoone, 1964) and in bis(glycylglycinato)zinc(II) dihydrate (Sandmark & Lindqvist, personal communication).

Relation to Cu^{II}*-binding by myoglobin*

The *p*H-dependence of the binding of Cu^{II} by myoglobin shows that histidyl side-chains are involved (Breslow & Gurd, 1963). The histidine residue at which the first Cu^{II} ion is bound has now been identified by the X-ray crystal study of Banaszak, Watson & Kendrew (1965). As in the carnosine complex, these authors show the Cu atom closest to the 3-nitrogen of the imidazole ring [Fig. 3(*b*) in their paper], and the remaining donor atoms belong to amino acid residues completely unconnected with the histidyl residue to whose imidazole ring the copper atom is bonded. On the other hand, in myoglobin these additional ligands are functional side chains and not peptide groups of the protein skeleton, the *p*H of crystallization being such that deprotonation of peptide nitrogen atoms would not be expected.

With one exception, the calculations were carried out on an IBM 7040 computer with the cooperation of Mr D. Richardson and the staff of the A.A.E.C. Computer Centre. The programs were written, or translated into FORTRAN IV, by Dr J. G. White and Dr B. M. Craven. The geometry of Fig. 2 was computed with a program written by Dr J. F. Blount, who later also produced Fig. 1 on the CDC 3600 computer of the C.S.I.R.O. Computing Research Section, Canberra. This research owes much to the helpful advice of Dr B. M. Craven, and to the comments of Professors J. T. Edsall, R. B. Martin, A. E. Martell and F. R. N. Gurd, who kindly read the draft manuscript. The work was supported by the Institute of General Medical Sciences, U.S. Public Health Service (Grant GM10867).

References

Banaszak, L. J., Watson, H. C. & Kendrew, J. C. (1965). *J. Mol. Biol.* **12**, 130.

Blount, J. F., Fraser, K. A., Freeman, H. C., Szymanski, J. T. & Wang, C.-H. (1967). *Acta Cryst.* **22**, 396.

Breslow, E. & Gurd, F. R. N. (1963). *J. Biol. Chem.* **238**, 1332.

Bryan, B. R., Poljak, R. J. & Tomita, K. (1961). *Acta Cryst.* **14**, 1125.

Bryce, G. F., Pinkerton, J. M. H., Steinrauf, L. K. & Gurd, F. R. N. (1965). *J. Biol. Chem.* **240**, 3829.

Bryce, G. F. & Gurd, F. R. N. (1966). *J. Biol. Chem.* **241**, 122.

Buerger, M. J. (1942). *X-ray Crystallography*. Chapter 20. New York: John Wiley.

Busing, W. R., Martin, K. O. & Levy, H. A. (1962*a*). Report ORNL-TM-305. Oak Ridge National Laboratory, Tennessee.

Busing, W. R., Martin, K. O. & Levy, H. A. (1962*b*). Report ORNL-TM-306. Oak Ridge National Laboratory, Tennessee.

Dauben, C. H. & Templeton, D. H. (1955). *Acta Cryst.* **16**, 841.

Dobbie, H. & Kermack, O. (1955). *Biochem. J.* **59**, 254.

Fraser, K. A., Long, H. A., Candlin, R. & Harding, M. M. (1965). *Chem. Comm.* p. 344.

Freeman, H. C. (1966). In *The Biochemistry of Copper*. Aisen, P., Blumberg, W. and Peisach, J., Eds. New York: Academic Press.

Freeman, H. C., Robinson, G. & Schoone, J. C. (1964). *Acta Cryst.* **17**, 719.

Freeman, H. C., Schoone, J. C. & Sime, J. G. (1965). *Acta Cryst.* **18**, 381.

Freeman, H. C. & Szymanski, J. T. (1965). *Chem. Comm.* p. 598.

Freeman, H. C. & Taylor, M. R. (1965). *Acta Cryst.* **18**, 939.*

Fridrichsons, J. & Mathieson, A. McL. (1962). *Acta Cryst.* **15**, 1065.

Hamilton, W. C. (1955). *Acta Cryst.* **8**, 185.

Harding, M. M. & Cole, S. J. (1963). *Acta Cryst.* **16**, 643.

International Tables for X-Ray Crystallography (1962*a*). Vol. III. Ref. 12, p. 208. Birmingham: Kynoch Press.

International Tables for X-Ray Crystallography (1962*b*). Vol. III. Ref. 67, p. 209. Birmingham: Kynoch Press.

Jarvis, J. A. J. & Wells, A. F. (1960). *Acta Cryst.* **13**, 1028.

Jose, P., Pant, L. M. & Biswas, A. B. (1964). *Acta Cryst.* **17**, 24.

Koltun, W. L., Fried, M. & Gurd, F. R. N. (1960). *J. Amer. Chem. Soc.* **82**, 233.

Kretzinger, R. H., Cotton, A. F. & Bryan, R. F. (1963). *Acta Cryst.* **16**, 651.

Langenbeck, W. (1925). *Ber. dtsch. chem. Ges.* **58**, 227.

Leberman, R. & Rabin, R. B. (1959). *Trans. Faraday Soc.* **55**, 1660.

Lenz, G. R. & Martell, A. E. (1964). *Biochemistry*, **3**, 750.

Lukton, A. & Sisti, A. (1961). *J. Org. Chem.* **26**, 617.

Martin, R. B. (1960). *J. Amer. Chem. Soc.* **82**, 6053.

* We take this opportunity of correcting a minor error in part III (Freeman & Taylor, 1965). The caption for Table 2 did not make it clear that the standard deviations of the positional coordinates were quoted in $Å \times 10^4$.

MARTIN, R. B. & EDSALL, J. T. (1960). *J. Amer. Chem. Soc.* **82**, 1107.
MAUNTHNER, M. (1913). *S. B. Akad. Wiss. Wien*, **122**, Abt. IIb, 269; *Mh. Chem.* **34**, 883.
NAKAMOTO, K. (1963*a*). *Infrared Spectra of Coordination Compounds*, p.206. New York: John Wiley.
NAKAMOTO, K. (1963*b*). *Infrared Spectra of Coordination Compounds*, p.204. New York: John Wiley.
ORGEL, L. E. (1960). *Introduction to Transition Metal Chemistry*, p.80. London: Methuen.
PROUT, C. K. & WISEMAN, T. J. (1964). *J. Chem. Soc.* p.497.
RABIN, B. R. (1956). *Trans. Faraday Soc.* **52**, 1134.
RABIN, B. R. (1958). In *Metals and Enzyme Activity*, p.21. Crook, E. M., Ed. Biochemical Society Symposia No.15, Cambridge Univ. Press.
ROSENBERG, A. (1956). *Acta Chem. Scand.* **10**, 840.
ROSENBERG, A. (1960). *Arch. Biochem. Biophys.* **88**, 83; *Biochim. Biophys. Acta*, **45**, 297.
ROSENBERG, A. (1961). *Ark. Kemi*, **17**, 25.
ROSSOTTI, F. J. C. & ROSSOTTI, H. (1961). *The Determination of Stability Constants*, p.40. New York: McGraw-Hill.
STRANDBERG, B., LINDQVIST, I. & ROSENSTEIN, R. (1961). *Z. Kristallogr.* **116**, 266.
TOMITA, K. (1961). *Bull. Chem. Soc. Japan*, **34**, 297.

Acta Cryst. (1967). **22**, 417

The Crystal Structure of $Rh_{17}Ge_{22}$, an Example of a New Kind of Electron Compound.

BY W. JEITSCHKO AND E. PARTHÉ

School of Metallurgical Engineering and Laboratory for Research on the Structure of Matter, University of Pennsylvania, Philadelphia, U.S.A.

(*Received* 16 *June* 1966)

$Rh_{17}Ge_{22}$ crystallizes with a tetragonal unit cell of unusual dimensions with $a=5{\cdot}604$, and $c=78{\cdot}45$ Å. One unit cell contains 68 Rh and 88 Ge atoms which are arranged in a new kind of 'superstructure'. The superstructure has two different substructures of different cell dimensions, one being formed by the Rh atoms, the other by the Ge atoms.

A number of structurally related transition metal silicides, germanides and gallides are known having the same pair of substructures but with different relative dimensions. It is shown that the relative subcell dimensions are controlled by the available valence electrons. These electron compounds offer a unique case where the relative valence electron contribution of the transition elements can be determined simply by a measurement of the X-ray diffraction line positions. The obtained values can then be used to calculate the compositions of new transition metal compounds.

Introduction

In the system rhodium–germanium there exist four different compounds: Rh_2Ge, Rh_5Ge_3, RhGe and a germanium rich phase. The crystal structures of the first three have been determined by Geller (1955). Zhuravlev & Zhdanov (1956) determined the composition of the fourth germanide as Rh_3Ge_4 and they reported also a tetragonal unit cell with $a=5{\cdot}7\pm0{\cdot}2$ and $c=10{\cdot}0\pm0{\cdot}3$ Å. In connection with earlier studies on the structure of the transition metal disilicides (Nowotny, Kudielka & Parthé, 1956; Duffin, Parthé & Norton, 1964), we found it of interest to study the crystal structure of the remaining rhodium germanide, which we expected initially to be a digermanide.

Experimental

The rhodium germanide needed for this investigation could be prepared by different methods. One method was to melt mixtures of elementary Rh and Ge in graphite crucibles under a purified Ar atmosphere in an induction furnace. Compressed powder mixtures were also melted without crucibles in an arc melting furnace. These methods produced a well crystallized material from which it was not difficult to pick appropriate single crystals. Microcrystalline material for powder diffraction patterns was obtained from Rh and Ge powder mixtures sintered in evacuated quartz tubes at 700° for 4 weeks. To avoid a violent initial reaction between the starting materials, it was found useful to raise the temperature gradually to 700°C over a week.

The presence of Ge lines in powder patterns of alloys composed as $RhGe_2$ indicated that the new phase was not a digermanide. X-ray and metallographic investigations of samples covering a range in Ge content showed that the true composition must be close to $RhGe_{1{\cdot}3}$ as suggested by Zhuravlev & Zhdanov (1956).

Powder and single-crystal diffraction techniques have been used for this structure study. For the determination of the crystal structure, intensities were recorded photographically with Mo $K\alpha$ radiation on a Nonius integrating Weissenberg camera using the multiple film technique and equi-inclination setting. To reduce the intensity of the diffracted beam we used copper foils of 0·001 inch thickness between the films. Very